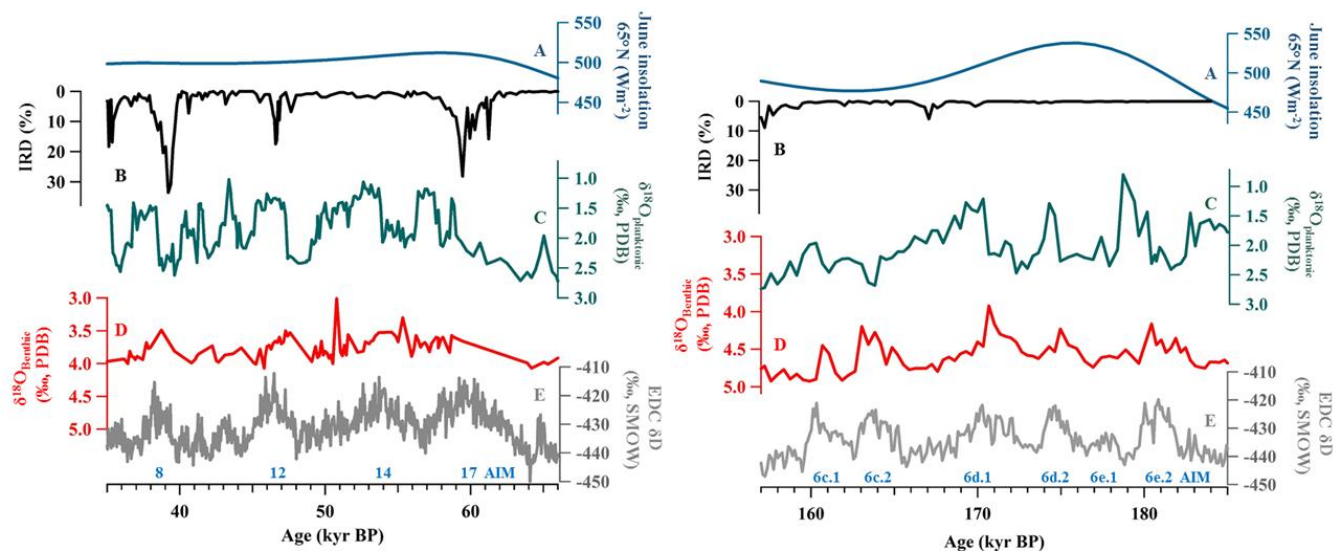


# Supplement Information of Millennial-scale atmospheric CO<sub>2</sub> variations during the Marine Isotope Stage 6 period (190-135 kyr BP)

Jinhwa Shin et al.,

5 Correspondence to: Jérôme Chappellaz ([jerome.chappellaz@univ-grenoble-alpes.fr](mailto:jerome.chappellaz@univ-grenoble-alpes.fr))



**Figure S1:** Comparison of climate related signals during MIS 3 (left) and 6 (right) period. A: 21 June insolation at 65°N (Berger, 1978). B: Ice-rafted debris (IRD) input in the Iberian margin core MD95–2040 (de Abreu et al., 2003). C:  $\delta^{18}\text{O}$  of planktonic foraminifera in the Iberian margin marine Core MD01–2444 (Margari et al., 2010). D:  $\delta^{18}\text{O}$  of Benthic foraminifera in the Iberian margin marine Core MD01–2444 (Margari et al., 2010). E: Temperature in Antarctica from  $\delta\text{D}$  composition of the EDC ice core (Jouzel et al., 2007).

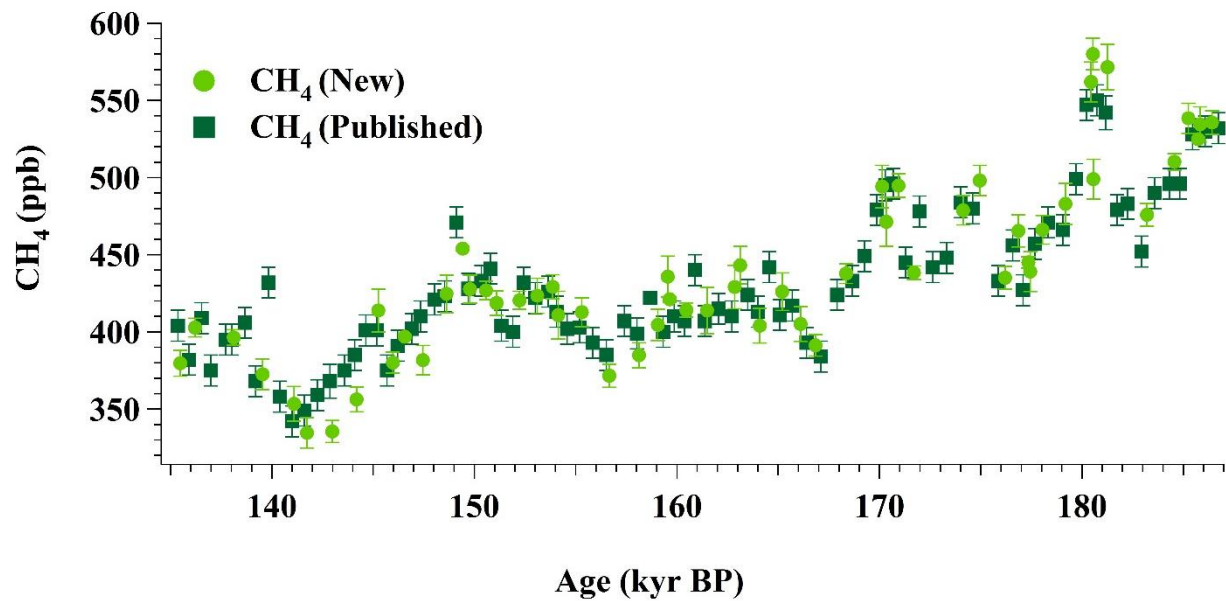


**Figure S2:** Atmospheric CH<sub>4</sub> concentrations from EDC ice core during MIS 6. Both the dark green squares (Louergue et al., 2008) and the light green dots (this study) were measured at IGE.

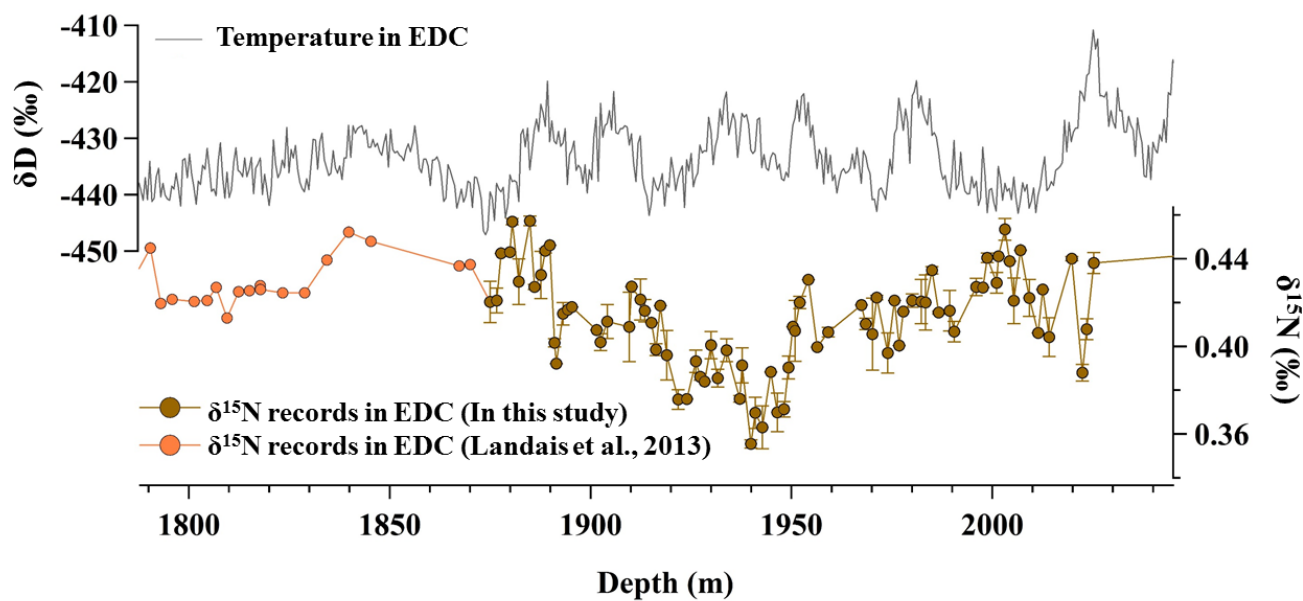


**Figure S3:**  $\delta D$  and  $\delta^{15}N$  from EDC ice core plotted as a function of depth. For  $\delta^{15}N$ , 88 new data points are added to the previous measurements (Landais et al., 2013). The error bar indicates the standard deviation of replicate measurements.

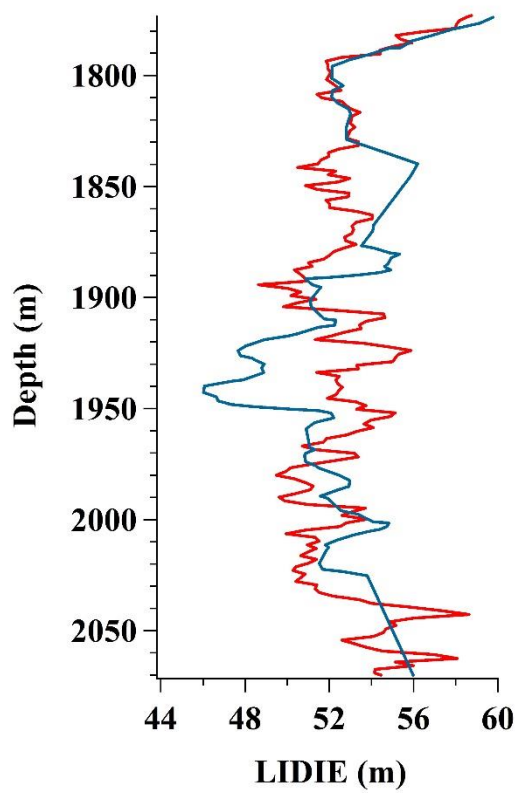


**Figure S4:** The Lock-In Depth in Ice Equivalent (LIDIE) calculated in AICC2012 (Bazin et al., 2013) and the LIDIE deduced from  $\delta^{15}\text{N}$  in this study.

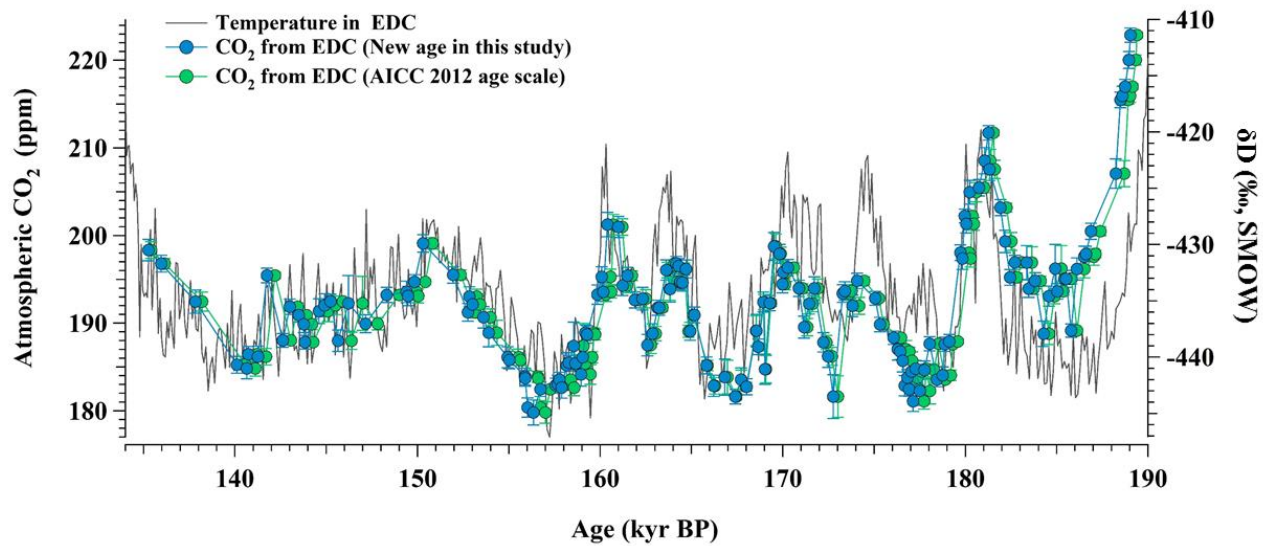


**Figure S5:** Blue dots: Atmospheric CO<sub>2</sub> from EDC on the revised AICC 2012 age scale. Green dots: Atmospheric CO<sub>2</sub> from EDC on the AICC 2012 age scale. Grey line: δD of water from EDC (temperature proxy) (Jouzel et al., 2007).

5

10

15

20

## Definition of the onset of abrupt climate change in the NH

Over the last glacial period, rapid CH<sub>4</sub> jumps were always synchronous with abrupt temperature increases in Greenland within  $\pm 50$  ppb (Huber et al., 2006). We pick intervals when CH<sub>4</sub> increases rapidly by at least 50 ppb over a time period of less than 1 kyr that correspond with Antarctic isotope maxima (Louergue et al., 2008). The timing of abrupt CH<sub>4</sub> increases was defined as the midpoint between the beginning of the increase of CH<sub>4</sub> and its maximum. The age uncertainty of the midpoint is defined

5 as the time difference between the beginning of the increase of CH<sub>4</sub> and its maximum. The age uncertainty of the midpoint is defined by the time difference between the midpoint and either of the two endpoints. We found three abrupt CH<sub>4</sub> increases during MIS 6 period at  $171.1 \pm 0.2$ ,  $175.4 \pm 0.4$  and  $181.5 \pm 0.3$  kyr BP (Figure S6). Due to the low accumulation rate and low temperature at the site during glacial periods, abrupt changes of CH<sub>4</sub> concentration might be smoothed, and identifying abrupt changes of CH<sub>4</sub> is more difficult than for interglacial periods. The climate change at 175.4 kyr BP does not seem to occur as abruptly as the other two, since CH<sub>4</sub> varied slowly over  $\sim 800$  years. However, we include this event because corresponding data of  $\delta^{18}\text{O}$  composition of planktonic foraminifera (Shackleton et al., 2000) indicate a rapid warming, and therefore an abrupt climate change in NH. Rapid increases during the last glacial period (MIS 3 and 5) are also calculated using this method to identify the onset of abrupt warming in NH. In total, eight changes are selected during this

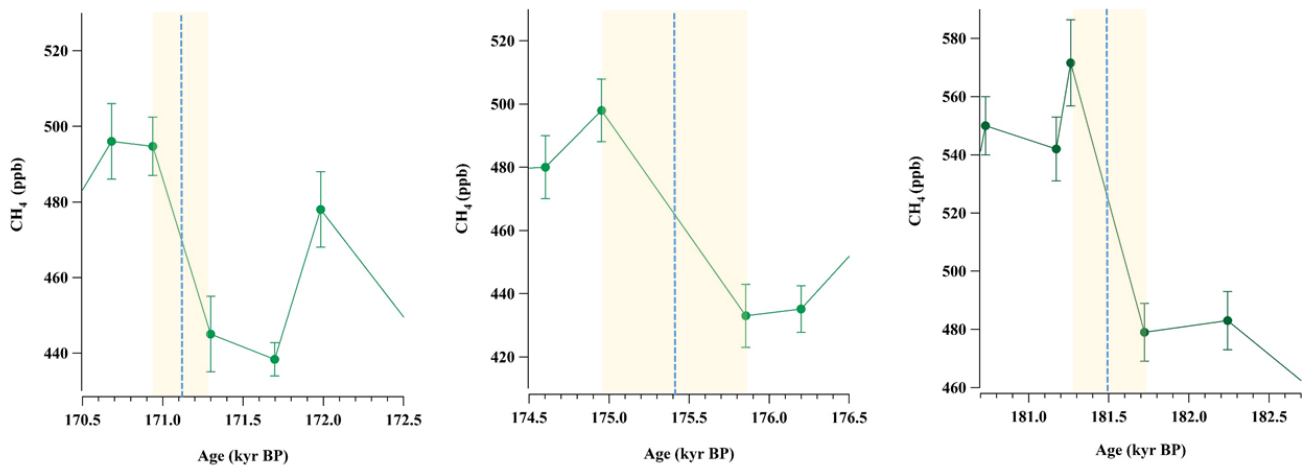


**Figure S6:** Atmospheric CH<sub>4</sub> records from EDC during MIS 6 period. Three boxes show CH<sub>4</sub> jumps at  $171.1 \pm 0.2$ ,  $175.4 \pm 0.4$  and  $181.5 \pm 0.3$  kyr BP.

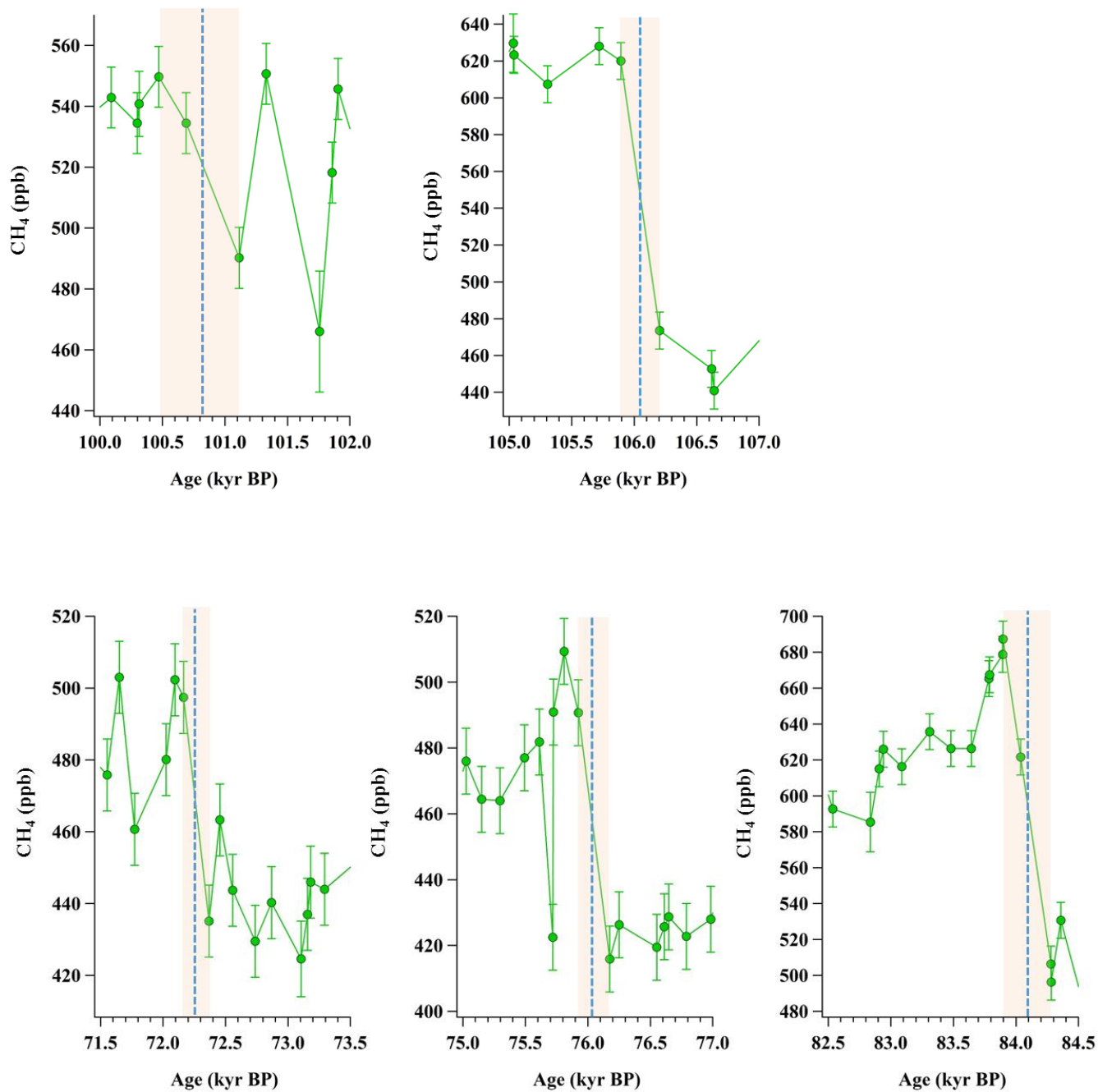


**Figure S7:** Atmospheric CH<sub>4</sub> records from EDML during the MIS 5 period. Two boxes show CH<sub>4</sub> jumps at  $72.3 \pm 0.1$ ,  $76.0 \pm 0.1$ ,  $84.1 \pm 0.2$ ,  $100.8 \pm 0.5$  and  $106.0 \pm 0.2$  kyr BP.

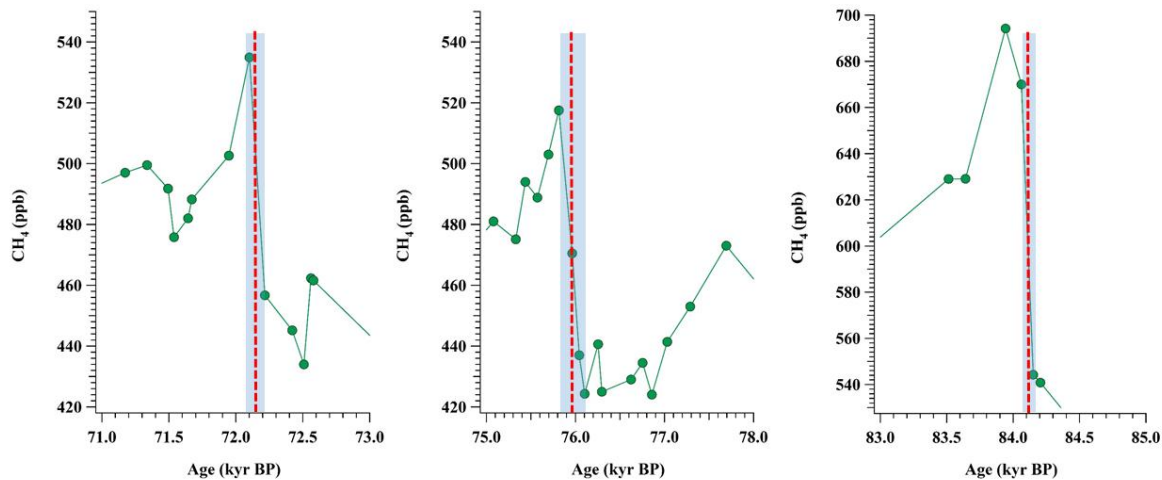


**Figure S8:** Atmospheric CH<sub>4</sub> records from the Byrd ice core during MIS 5 period. Three boxes show CH<sub>4</sub> jumps at  $72.2 \pm 0.1$ ,  $76.0 \pm 0.2$  and  $84.1 \pm 0.04$  kyr BP.

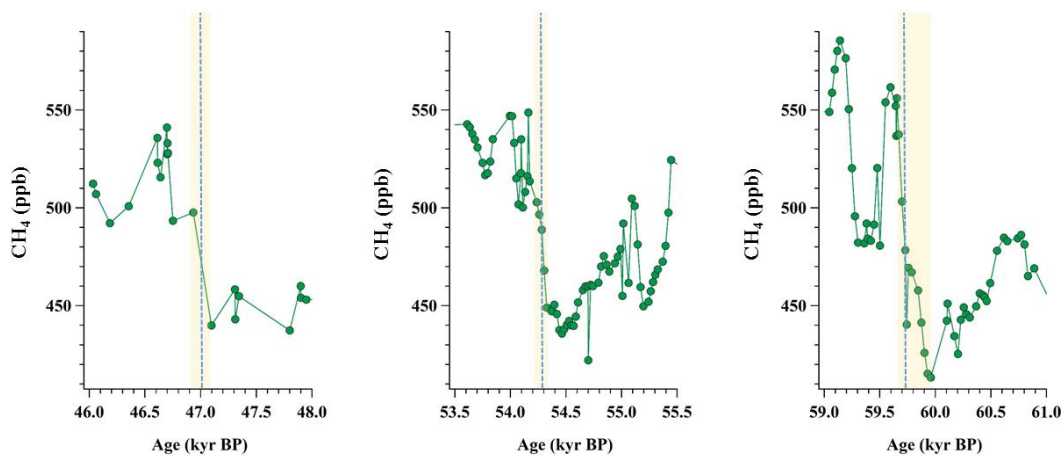


**Figure S9:** Atmospheric CH<sub>4</sub> records from TALDICE during MIS 3 period. Three boxes show CH<sub>4</sub> jumps at  $46.7 \pm 0.2$ ,  $54.2 \pm 0.1$  and  $59.7 \pm 0.1$  kyr BP.



## Definition of minima and maxima of atmospheric CO<sub>2</sub>

A two-steps procedure was used in order to select the maxima and minima of CO<sub>2</sub> concentrations during the penultimate glacial periods, and calculate the associated age uncertainty (Figure S10 and Table S1). First, inflection points were selected by finding zero values in the second Savitsky–Golay filtered derivative of the data. The parameters of the Savitsky–Golay filters were chosen in order to remove sub–millennial scale variations. We use the same parameters for MIS 3, MIS 5 and 6. Second, a Monte Carlo simulation was conducted, in which the original data were resampled within their uncertainty, and the absolute minima and maxima between pairs of inflection points were selected. This allows us to assign an approximate uncertainty to the timing of each minimum/maximum. The square of the age uncertainty associated with sampling (taken to be the mean sampling resolution) was added to the squared uncertainty calculated in the Monte Carlo procedure to calculate a total uncertainty value.

**Table S1:** The minima and maxima locations of atmospheric CO<sub>2</sub> during the MIS 6.

	CDM 6c.1			CDM 6c.2			CDM 6d.1			CDM 6d.2			CDM 6e.2		
	Min	Max	Min	Min	Max	Min	Min	Max	Min	Min	Max	Min	Min	Max	Min
Age (kyr BP)	156.3	160.6	162.6	162.6	164.2	167.2	167.2	169.6	172.7	172.7	174.1	177.2	177.2	181.3	184.9
2 $\delta$ (kyr BP)	0.3	0.3	0.2	0.2	0.3	0.5	0.5	0.2	0.2	0.2	0.2	0.3	0.3	0.2	0.8

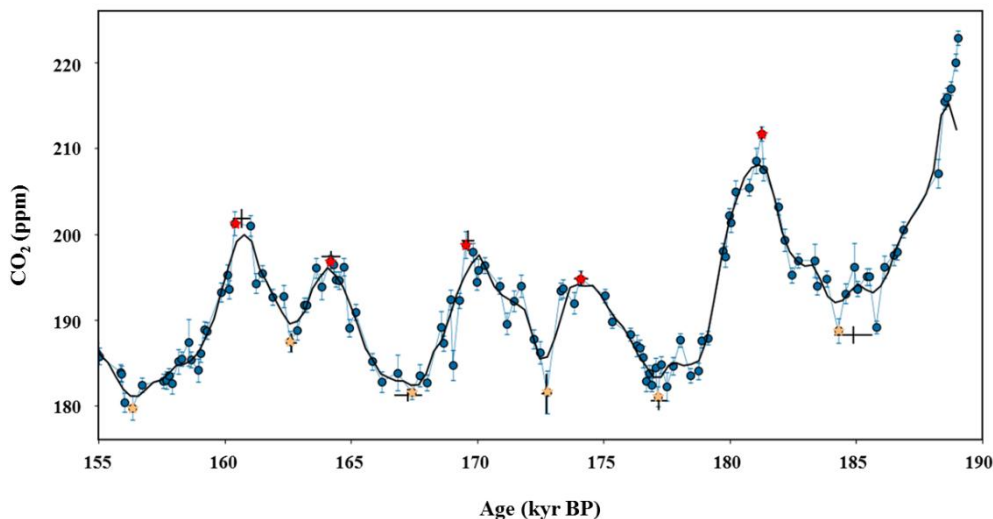


**Figure S10:** The red and yellow points are the minimum/maximum measured points of atmospheric CO<sub>2</sub> during MIS 6 respectively. Blue dots indicate atmospheric CO<sub>2</sub>. The bars indicate the timing and CO<sub>2</sub> uncertainty for each minimum/maximum.

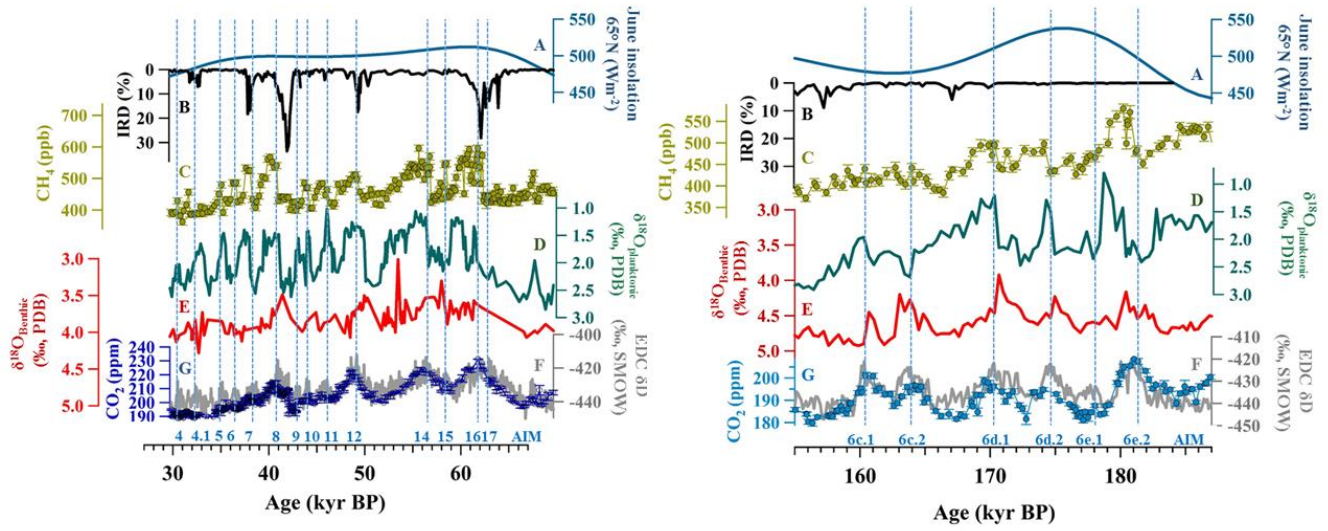


**Figure S11:** Comparison of climate with atmospheric CO<sub>2</sub> during MIS 3 (left) and 6 (right) period. A: 21 June insolation at 65°N (Berger, 1978). B: Ice-rafted debris (IRD) input in the Iberian margin core MD95–2040 (de Abreu et al., 2003). C: Atmospheric CH<sub>4</sub> in EDC during MIS 3 (Loulergue et al., 2008) and composite data of atmospheric CH<sub>4</sub> in EDC during MIS 6 (Loulergue et al., 2008; this study). D: δ<sup>18</sup>O of planktonic foraminifera in the Iberian margin marine Core MD01–2444 (Margari et al., 2010). E: δ<sup>18</sup>O of Benthic foraminifera in the Iberian margin marine Core MD01–2444 (Margari et al., 2010). F: Temperature in Antarctica from δD composition of the EDC ice core (Jouzel et al., 2007). G: Composite data of atmospheric CO<sub>2</sub> in Antarctic ice cores during MIS 3 (Bereiter et al., 2015) and atmospheric CO<sub>2</sub> in EDC during MIS 6 (this study). Dashed lines indicates the timing of AIM events. The numbers of AIM events are written at the bottom of the dashed lines.

5

10

15

## References

- Bazin, L., Landais, A., Lemieux-Dudon, B., Kele, H. T. M., Veres, D., Parrenin, F., Martinerie, P., Ritz, C., Capron, E., and Lipenkov, V.: An optimized multi-proxy, multi-site Antarctic ice and gas orbital chronology (AICC2012): 120-800 ka, *Clim. Past*, 9, 1715-1731, 2013.
- 5 Bereiter, B., Eggleston, S., Schmitt, J., Nehrbass-Ahles, C., Stocker, T. F., Fischer, H., Kipfstuhl, S., and Chappellaz, J.: Revision of the EPICA Dome C CO<sub>2</sub> record from 800 to 600 kyr before present, *Geophys. Res. Lett.*, 42, 542-549, 2015.
- Berger, A. L.: Long-Term Variations of Caloric Insolation Resulting from the Earth's Orbital Elements 1, *Quat. Res.*, 9, 139-167, 1978.
- 10 de Abreu, L., Shackleton, N. J., Schönfeld, J., Hall, M., and Chapman, M.: Millennial-scale oceanic climate variability off the Western Iberian margin during the last two glacial periods, *Mar. Geol.*, 196, 1-20, 2003.
- Jouzel, J., Masson-Delmotte, V., Cattani, O., Dreyfus, G., Falourd, S., Hoffmann, G., Minster, B., Nouet, J., Barnola, J.-M., and Chappellaz, J.: Orbital and millennial Antarctic climate variability over the past 800,000 years, *Science*, 317, 793-796, 2007.
- 15 Landais, A., Dreyfus, G., Capron, E., Jouzel, J., Masson-Delmotte, V., Roche, D., Prié, F., Caillon, N., Chappellaz, J., and Leuenberger, M.: Two-phase change in CO<sub>2</sub>, Antarctic temperature and global climate during Termination II, *Nat. Geosci.*, 6, 1062, 2013.
- Loulergue, L., Silt, A., Spahni, R., Masson-Delmotte, V., Blunier, T., Lemieux, B., Barnola, J.-M., Raynaud, D., Stocker, T. F., and Chappellaz, J.: Orbital and millennial-scale features of atmospheric CH<sub>4</sub> over the past 800,000 years, *Nature*, 453, 20 383, 2008.
- Margari, V., Skinner, L., Tzedakis, P., Ganopolski, A., Vautravers, M., and Shackleton, N.: The nature of millennial-scale climate variability during the past two glacial periods, *Nat. Geosci.*, 3, 127, 2010.
- Shackleton, N. J., Hall, M. A., and Vincent, E.: Phase relationships between millennial-scale events 64,000–24,000 years ago, *Paleoceanography*, 15(6), 565-569, 2000.

25